Quantification of Hypotony Maculopathy Using Spectral-Domain Optical Coherence Tomography

Rémy Dumas, MSc,† Magaly Lacourse, MD,*‡ Rabea Kassem, MD,* Mark R. Lesk, MSc, MD,*‡ and Santiago Costantino, PhD*‡*

Précis: We provide a free-to-use, open-source algorithm to quantify macular hypotony based on optical coherence tomography (OCT) images. This numerical approach calculates a metric that measures the deviations of Bruch's membrane from a smooth ideal retinal layer.

Purpose: Hypotony maculopathy is a recurrent complication of glaucoma surgical interventions in which extremely low intraocular pressure triggers changes in the shape of retinal layers. Abnormal folds can often be observed in the retina using standard fundoscopy, but OCT is particularly important to appreciate the severity of symptoms at different depths. Despite the need for metrics that could be used for the informed clinical decision to evaluate the progression and resolution of macular hypotony, algorithms that quantify the retinal folds are not available in the literature or included in clinical imaging equipment. The purpose of this work is to introduce a simple algorithm that can be used to assess hypotony maculopathy from OCT B-Scans and volumes and a free, open-source implementation.

Methods: The pipeline we present is based on a straightforward segmentation of Bruch's membrane complex. The principal idea of quantification is to compute a smoothed version of this complex and analyze the deviations from an ideal interface. Such deviations are then measured and added to create a metric that characterizes each OCT B-Scan. A full OCT volume reconstruction is thus characterized by the average metric obtained from all planes.

Results: We tested the metric we proposed against the assessment of 3 experts and obtained a very good correspondence, with Pearson correlation coefficients higher than 0.8. Furthermore, agreement with automatic analysis seemed better than between experts. We describe the pipeline in detail and illustrate the results with a group of patients, comparing baseline images, severe hypotony maculopathy, and a variety of outcomes.

Conclusion: The tool we introduce and openly provide fills a clinical gap to quantitatively grade hypotony maculopathy. It offers a metric of relatively simple interpretation that can be used to help clinicians in cases where the regression of symptoms is not obvious to the naked eye. Our pilot study demonstrates reliable results, and an open-source implementation facilitates easy improvements to our algorithm.

Key Words: hypotony maculopathy, optical coherence tomography, glaucoma, filtering surgery, SANS, image processing

(*J Glaucoma* 2023;32:287–292)

Hypotony maculopathy (HM) is a serious complication of glaucoma filtering surgeries that can lead to permanent vision loss. The incidence of this complication has been reported to occur in up to 20% of the filtering surgeries, and the wide use of antimetabolites has exacerbated their prevalence.[1–3] HM, despite its name, affects the entire fundus and is characterized by chorioretinal folds that radiate outward from the fovea, vascular tortuosity, edema of the optic nerve head, and hyperopic shift.[2] A similar clinical picture is found in Spaceflight Associated Neuro-Ocular Syndrome, which occurs in astronauts when subjected to prolonged weightlessness and which is a major impediment to deep space exploration and long-term missions.[4]

Spectral-domain optical coherence tomography (SD-OCT) is the most adequate tool for visualization of the folds of retinal pigment epithelium (RPE)/Bruch's membrane (BM) complex, which is the most characteristic clinical sign of HM.[5,6] OCT B-Scans acquired in the direction perpendicular to the folds (which are predominantly horizontal) minimize the chances of missing HM when scanning the posterior pole.[2] OCT is used for diagnosing HM and assessing resolution of the chorioretinal folds with normalization of the intraocular pressure (IOP), and is particularly important in patients that have subclinical HM and reduced visual acuity (VA), as hypotony with a normal fundus examination may not suffice to detect subtle retinal or choroidal folds.[7] A recent cross-sectional study reporting on the frequency of post glaucoma filtering surgery HM diagnosed 17 eyes with HM on SD-OCT images, but only 3 of those eyes were also diagnosed with fundus photography, further enhancing the crucial role of deep imaging in subclinical cases.[6]

Prior work to characterize the degrees of folding and distortion of the macular architecture to quantify and grade HM is either subjective or based on screen rulers,[8,9] thus an objective assessment of RPE/BM complex to accurately and reproducibly quantify chorioretinal folds on OCT images is lacking. Here, we describe an automatic RPE/BM complex segmentation algorithm for OCT retinal images and a new metric for the quantification of such folds. A free, open-source implementation of the algorithm is also provided.

MATERIAL AND METHODS

This study followed the tenets of the Declaration of Helsinki and was approved by the Maisonneuve-Rosemont Hospital institutional review board.

Received for publication May 19, 2022; accepted November 25, 2022.
From the *Maisonneuve-Rosemont Hospital Research Center; †École Polytechnique de Montréal; and ‡Department of Ophthalmology, University of Montreal, Montreal, QC.
This paper was supported by the following grants: Canadian Institutes of Health Research to SC and MRL, Fonds de Recherche du Québec - Santé to SC, Canadian Space Agency to SC and MRL, Fonds de Recherche en Ophtalmologie de l'Université de Montréal to MRL.
Disclosure: The authors declare no conflict of interest.
Reprints: Santiago Costantino, PhD, Université de Montréal, Montreal, QC Canada (e-mail: santiago.costantino@umontreal.ca).

DOI: 10.1097/IJG.0000000000002161

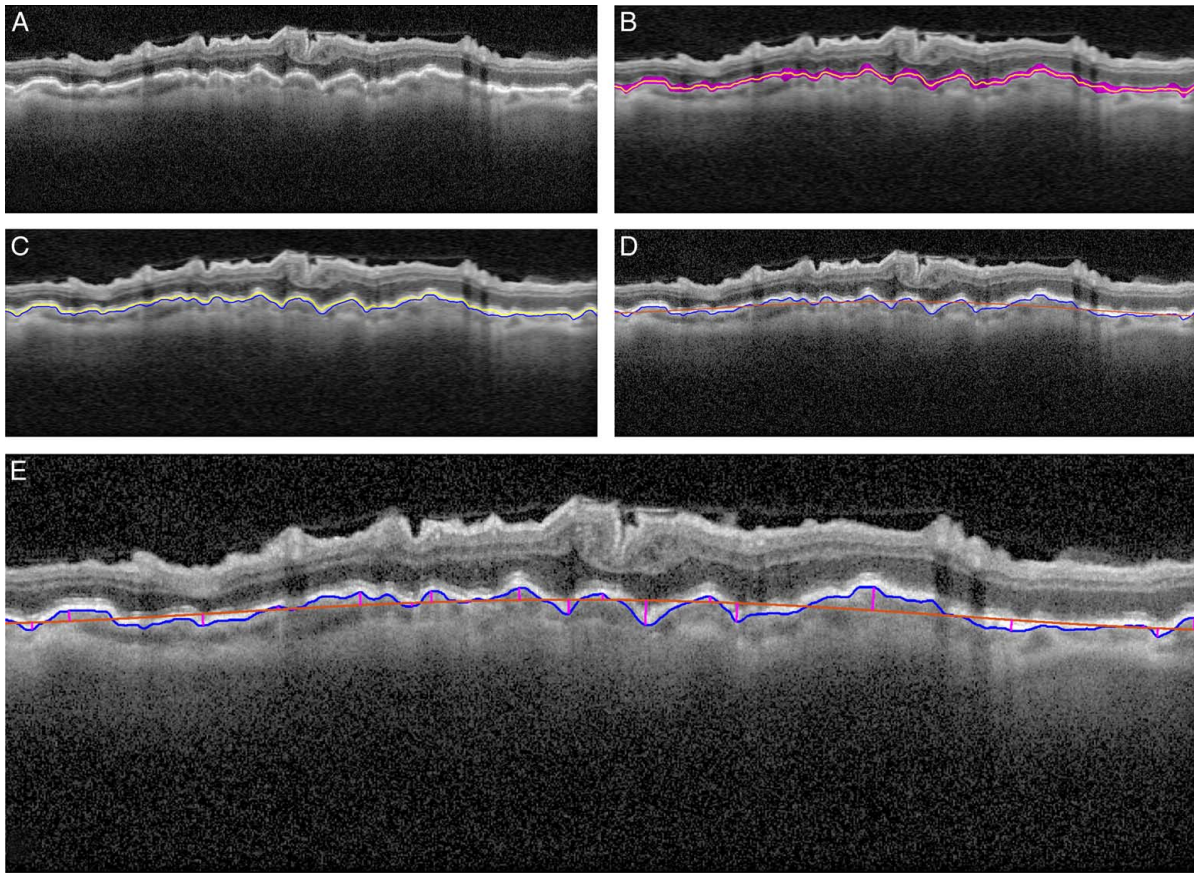

FIGURE 1. Illustration of Bruch's membrane segmentation algorithm. A, Original image OCT image. B, Image after filtering with a Gaussian kernel, and an approximation of the retina pigment epithelium (RPE, magenta) and its midline (yellow). C, Final Bruch's membrane (BM) complex (blue) located beyond the RPE midline (yellow). D, Polynomial approximation (orange) of the BM (blue) to make the folds apparent. E, Detected folds to extract their properties (height in magenta). Figure 1 can be viewed in color online at www.glaucomajournal.com.

Twenty-four patients with HM following a filtering glaucoma surgery were enrolled. Subjects were excluded if they had corneal, lens, or media opacities and unsteady fixation that resulted in poor retinal OCT quality. Their medical charts were reviewed to obtain their demographics and their medical, ocular, and surgical history. Their OCT images from various visits form the basis for all analyses performed in this study.

Definition of a Hypotony Maculopathy Metric

Spectral-domain OCT images (Spectralis SD-OCT, Heidelberg Engineering GmbH) are automatically segmented to measure different parameters of the RPE/BM complex. More specifically, our custom segmentation algorithm provides a precise detection of the oscillations displayed by the RPE/BM complex, deviating from a smooth layer. Based on clinical observations, our objective was to measure the area of these deviations from an ideal smooth interface to create a metric that highlights sharp folds more than smooth discrepancies. This metric is calculated for each B-Scan independently, and summed values are assigned to OCT volume reconstructions. The algorithm has 2 main parts: (A) Segmentation of the BM using a modified version of the method described in Mazzaferri et al[10,11] and (B) Measurements of the choroidal folds and computation of a HM metric.

BM segmentation (Fig. 1) is obtained by first minimizing speckle noise with a Gaussian filter. The filter size (1×10 pixels and SD $\sigma = 5$) was meant to avoid losing information of the boundary locations in the blurred image. The vertical gradient image typically shows peaks corresponding to the ILM, the anterior boundary of the RPE complex, and its posterior boundary, and they appear in order. To remove the outliers, a median filter is applied on each boundary to build references from which large deviations could be detected and eliminated. These

TABLE 1. The Performance of the Algorithm Was Tested With 3 Experts on a Set of 50 Images of Different Grades of Hypotony Maculopathy

	Expert A	Expert B	Expert C	Algorithm
Expert A	1	0.8840	0.7960	0.8449
Expert B	0.8840	1	0.8394	0.9076
Expert C	0.7960	0.8394	1	0.8313
Algorithm	0.8449	0.9076	0.8313	1

Inter-operator grading correlation show agreement between users and the algorithm is practically equivalent.

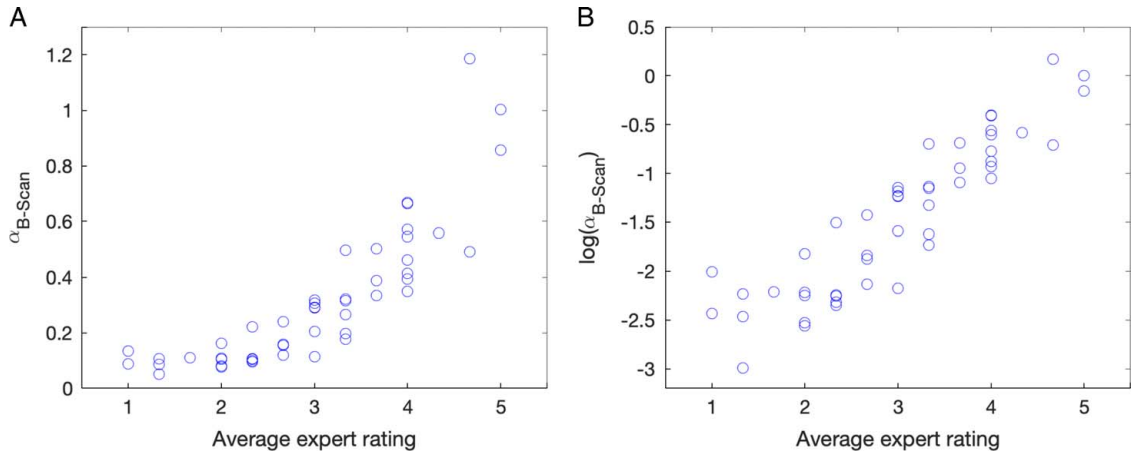

FIGURE 2. Comparison of the quantitative metric with clinician appreciation in (A) linear and (B) logarithmic scales for a set of 50 images with various degrees if hypotony maculopathy. Figure 2 can be viewed in color online at www.glaucomajournal.com.

points are interpolated to define the anterior and posterior boundaries of the RPE, and the highest intensity pixels of the original image in this region delineate the RPE midline. Posterior to the RPE midline, on each A-Scan, the locations of the 3 highest values on the absolute gradient image are averaged to give the BM position. As the last step, the trace is interpolated using the nearest neighbors to return the final BM. The analysis script and the implementation provided were coded in Matlab, and are available in GitHub (https://github.com/santiago-costantino/HMAlpha).

Folds are defined as the area between the segmented BM and a smoothed version of this layer obtained with a fit. The BM is thus fitted with a fourth-degree polynomial (Fig. 1E), and pixels between the polynomial fit and the BM as detected are defined as abnormal regions. The BM intersects its polynomial fit at several locations, and individual folds are defined as the surface between both curves limited by consecutive locations where both curves cross. For each one of these folds, we compute their width, height, and area. The width is defined as the Euclidean distance between intersecting points, and the height as the maximum separation from the BM fit to the segmented BM.

We defined a metric α that characterizes a full B-Scan using the sum of the areas of all folds detected. This metric weights the folds differently considering their sharpness, so that steep folds contribute more to the sum than shallow folds. More explicitly, the score α for a B-Scan with N detected folds is:

$$\alpha_{B-Scan} = \frac{1}{W}\sum_{i}^{N} s_i \frac{h_i}{w_i},$$

where W is the total width of tissue analyzed in the B-Scan, s_i is the area of fold i, h_i and w_i are their height and width, respectively.

For a complete OCT volume composed of M B-Scans, the metric is simply the average of all α_{B-Scan} in the series:

$$\alpha_V = \frac{1}{M}\sum_{j}^{M} \alpha_{B-Scan_j}.$$

RESULTS

The mean age of patients was 68 ± 16 y. Mean IOP before surgery was 28 ± 14 and during HM was 5.0 ± 2.4 mm Hg. Mean VA before HM was 0.69 ± 0.29 and during HM (pinhole) was 0.49 ± 0.27.

We validated our method using 50 randomly selected B-Scans from a data set of 36 volumes derived from the 24 patients included in this study and compared our results with the assessment of 3 experts. Two fellowship-trained glaucoma specialists and 1 PhD biophysicist with 15 years of experience in OCT image analysis involving glaucoma and retinal disease were asked to rate the severity of the condition from 1 (healthy) to 5

TABLE 2. Three Timepoints on 5 Cases Are Illustrated

	IOP (mm Hg)			Visual acuity (20/×)			α_V		
Patient	**Pre**	**HM**	**Post**	**Pre**	**HM**	**Post**	**Pre**	**HM**	**Post**
1	34	3	17	20	200	20	0.13	1.16	0.11
2	33	4	13	20	60	20	0.23	1.02	0.32
3	3	3	7	100	400	20	0.43	0.97	0.13
4	43	5	10	50	400	70	0.3	5.79	3.22
5	9	3	14	20	70	20	0.2	2.73	0.97

The metric alpha displays the evolution of the disease based on Retinal pigmented epithelium/Bruch's membrane complex measurements of the entire OCT volume by our automated segmentation algorithm on patients with hypotony maculopathy following glaucoma filtering.

(diseased). The images, which were a mix of both vertical and horizontal scans, were extracted and presented without identifiers.

The automated metric was compared with the individual ratings and to the average rating. Table 1 shows the inter-operator Pearson correlations to indicate the human variability for this task on our selection of 50 B-Scans. Experts' opinions agree more with our algorithm than they do with those of their colleagues. The average rating assigned by experts displays a Pearson correlation of 0.84 with $\alpha_{B\text{-}Scan}$ and of 0.91 with $\log(\alpha_{B\text{-}Scan})$, as displayed in Figure 2.

To illustrate how this metric evolves as the disease progresses, we show 5 cases. A description of the baseline characteristics and chorioretinal folds parameters measured by our automated segmentation algorithm in this study is presented in Table 2 and plotted in Figure 3. Figure 4 shows single B-Scans extracted from the volumes used in Table 2, at baseline and during their evolution. We note that our automated metric tracks well the evolution of these clinical cases.

The Pearson coefficient correlation of α_v versus VA was significant ($R = -0.56$, $P = 0.02$) while α_v versus IOP was not ($R = -0.39$, $P = 0.16$). In our data set, the α_v values for nonhypotonous eyes fell below 0.5 μm while the HM values fell between 1.0 and 6 μm.

DISCUSSION

We propose a simple approach to quantify a common complication of filtration surgery. It consists of a parameter with a relatively straightforward interpretation derived from deviations from an idealized smooth RPE/BM complex. In a nutshell, if we consider the total area S of all folds in an image, $\alpha_{B\text{-}Scan}$ represents the height of a rectangle of surface S and the same width as the image W. The height $\alpha_{B\text{-}Scan}$ of such a rectangle is still an approximation because the individual folds are weighted using their shape, but the overall value is adequately representative. To facilitate the adoption and evaluation of the metric, we provide an open-source, free-to-use implementation and a compiled version of the software, to quantify HM on both single images and full-volume OCT reconstructions. Since the metric is not dependent on this particular segmentation strategy and can eventually be adapted to better-performing algorithms, an open-source implementation opens the door to straightforward improvements.

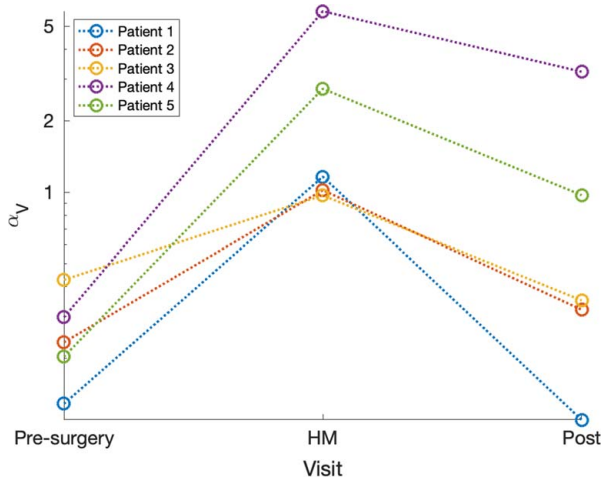

FIGURE 3. Illustration of 5 hypotony maculopathy cases evolution and their alpha metric. Figure 3 can be viewed in color online at www.glaucomajournal.com.

Segmentation errors that may directly affect the final metrics $\alpha_{B\text{-}Scan}$ and α_{Volume} were rare, found only in very low signal-to-noise ratio images. The mistakes we observed were too small or isolated to single bad-quality images to have any significant effect on the overall quantification of the disease. In some cases, especially for severely diseased eyes, where BM displays holes and discontinuities are common, individual folds can be missed. However, even in these problematic cases, quantification based on the correctly segmented fraction provides a fair assessment of the condition.

A nonlinear relation between the metric α and expert assessment can be observed in Figure 2A, where a logarithmic scale seems to represent better human insight. This is likely due to a perception issue, in a way often referred as Weber-Fechner law,[12] as small deviations captured by α seem to be amplified by clinicians' appreciation. It is too early to say whether this nonlinear relationship has any clinical implications, but it is important to highlight this interesting observation.

The fact that the agreement of experts with automatic segmentation is higher than that with other evaluators must be appraised considering that only 5 integer possible values were available to clinician experts, while the algorithm was not so restricted. However, if we round the output of our metric into 5 groups with equal amounts of images, correlations still range from 0.80 to 0.84.

The metric α represents a local description of the examined section of the fundus. It describes the folds in OCT images and volumes normalized to the size of the tissue section examined. Thus, corrections that take into consideration the magnitude on the regions of interest analyzed in every patient and location in the fundus may be required for larger studies.

Tissue folds are also present on ILM. Indeed, sometimes the ILM is more affected by the disease than the BM. Extending the calculation of folds to the neuronal layers is straightforward using the open-source implementation provided. Nevertheless, a low-degree polynomial fit is not always adequate to address the profile of the retina-vitreous interface at the fovea, as this sometimes yields artifactual deviations from a smooth surface and was not considered in this pilot study but still available in the implementation provided.

Quantitative assessment of macular folds in Spaceflight Associated Neuro-Ocular Syndrome will help us to better understand the risk factors for this disorder, especially since only small numbers of astronauts can be studied. Similarly, while some risk factors for hypotony maculopathy are understood,[2,3,7] it remains difficult to predict who is most likely to develop it and at what IOP. In our study, α_v seemed to correlate better with VA than with IOP, which makes sense given that low IOP does not always cause HM. Indeed, even after severe reduction of postsurgery IOP HM is not always observed, whereas folds in the photoreceptor layer will necessarily yield VA reduction. A tool to quantitatively assess the spectrum of HM will facilitate studies aimed at understanding known risk factors and discovering others to ultimately allow us to predict which eyes are at greatest risk before surgery. This information may allow us to modify our surgical approach to avoid this disorder.

As is, the new metric provides a novel tool to help clinical decisions that today lack adequate technologies.

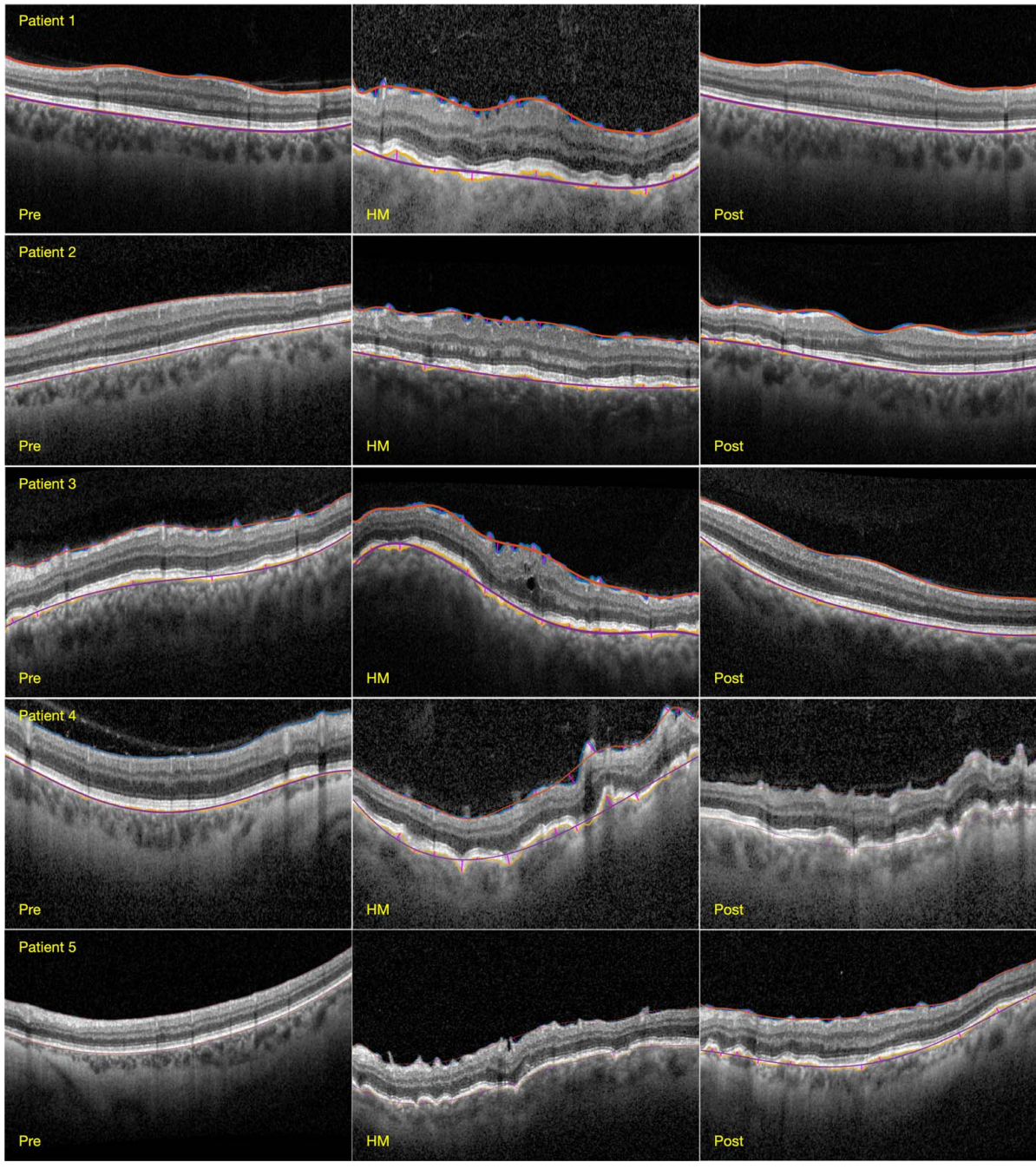

FIGURE 4. Single B-Scans extracted from the volumes used in Table 2. Patients 1, 2, and 4 are shown before trabeculectomy at baseline. Patients 3 and 5 are shown years after trabeculectomy. ("Pre"), before severe HM developed following the development of bleb leaks. Patient 3 had mild HM at baseline. All patients are shown "Post" following surgical repair of the filtration bleb. Figure 4 can be viewed in color online at www.glaucomajournal.com.

Quantitative evaluation of HM improvement that would delay or precipitate follow-up surgical interventions will be improved with precise algorithms that assess the changes in the macular health. Providing the source code and a free implementation will allow widespread evaluation of the technique, which will ultimately determine its value in the clinical setting. Future studies could use this novel parameter, applied to both the outer and inner retina, to better understand the role of outer retinal folds, inner retinal folds, and various degrees and patterns of HM in determining visual function.

REFERENCES

1. Abbas A, Agrawal P, King AJ. Exploring literature-based definitions of hypotony following glaucoma filtration surgery and the impact on clinical outcomes. *Acta Ophthalmol*. 2018;96:e285–e289.
2. Costa VP, Arcieri ES. Hypotony maculopathy. *Acta Ophthalmol Scand*. 2007;85:586–597.

3. Rabiolo A, Leadbetter D, Anand N. Hypotony-associated complications after deep sclerectomy: incidence, risk factors, and long-term outcomes. *J Glaucoma*. 2021;30:e314–e326.
4. Wojcik P, Kini A, Al Othman B, et al. Spaceflight associated neuro-ocular syndrome. *Curr Opin Neurol*. 2020;33:62–67.
5. Edwards Mayhew RG, Kahook MY, Seibold LK. Hypotony maculopathy captured with vertical rasters on optical coherence tomography (OCT) imaging. *Am J Ophthalmol Case Rep*. 2021;22:101076.
6. Azuma K, Saito H, Takao M, et al. Frequency of hypotonic maculopathy observed by spectral domain optical coherence tomography in post glaucoma filtration surgery eyes. *Am J Ophthalmol Case Rep*. 2020;19:100786.
7. Thomas M, Vajaranant TS, Aref AA. Hypotony maculopathy: clinical presentation and therapeutic methods. *Ophthalmol Ther*. 2015;4:79–88.
8. Soneru AR, Shah S, and Tanna AP. *Classification System for Hypotony Maculopathy*. in *ARVO Annual Meeting Abstract*. 2016.
9. Raja M, Boukavala S, Goldsmith C, et al. Spectral domain OCT to diagnose clinically inapparent hypotony maculopathy using 3D image rendering software. *BMJ Case Rep*. 2012;2012: bcr2012007842.
10. Mazzaferri J, Beaton L, Hounye G, et al. Open-source algorithm for automatic choroid segmentation of OCT volume reconstructions. *Sci Rep*. 2017;7:42112.
11. Beaton L, Mazzaferri J, Lalonde F, et al. Non-invasive measurement of choroidal volume change and ocular rigidity through automated segmentation of high-speed OCT imaging. *Biomed Opt Express*. 2015;6:1694–1706.
12. Kandel ER, Jessell TM, Schwartz JH, et al, *Principles of neural science*. 2013.

Copyright © 2022 Wolters Kluwer Health, Inc. All rights reserved.